Available online at www.sciencedirect.com

ScienceDirect

IFAC Papers Online CONFERENCE PAPER ARCHIVE

IFAC PapersOnLine 56-2 (2023) 2671–2676

# Free-form Bending Control using Optimal Residual Strategies ⋆

**Ahmed Ismail** * **Daniel Maier** ** **Sophie Stebner** *** **Sebastian Münstermann** *** **Wolfram Volk** ** **Boris Lohmann** *

* *Chair of Automatic Control, Technical University of Munich, Boltzmannstr. 15, 85748 Garching, Germany (Tel: +49 (89) 289 -15664; e-mail: a.ismail@tum.de).*

** *Chair of Metal Forming and Casting, Technical University of Munich, Walther-Meißner-Str. 4, 85748 Garching, Germany (e-mail: daniel.maier@utg.de)*

*** *Integrity of Materials and Structures, RWTH Aachen University, Intzestr. 1, 52072 Aachen, Germany (e-mail: sophie.stebner@iehk.rwth-aachen.de)*

**Abstract:** Free-form bending is a bending technique, whereas the bending tool head combines both linear and rotary motions. One problem with free-form bending is that an incorrectly bent tube section can no longer be corrected. Therefore, if a defect is detected during bending, a strategy for bending the remaining tube sections must be determined in such a way that the overall shape of the tube is as close as possible to the desired one. In this paper, a solution based on optimal recalculation of the residual trajectories of the bending tool head is presented and different cost functions are discussed in terms of their effect on the overall shape. Simulation results have shown a significant improvement of the resulting end shape of the workpiece upon subjecting it to perturbation.



*Keywords:* Process modelling, Advanced process control, Process Optimization, Soft sensors, Freeform bending

## 1. INTRODUCTION

Free-form bending is a relatively new bending technology, which allows for the bending of complex geometries without the need to change the bending tool (see Fig. 1). Here, a worker inserts the pipe into the machine, which then gets pushed forward through the bending head, while the bending head moves linearly and/or rotationally. The applications for free-form bending are diverse, ranging from transport (i.e., the automotive industry and shipbuilding), aerospace engineering, power plants, and even medicine as in Huang et al. (2019); Ahn et al. (2020); Zhang et al. (2022).

### *1.1 State of the Art*

In the past, the application of classical control paradigms in the field of free-form bending was focused only on guaranteeing that the trajectory path of the bending head is not deviated from a desired precalculated path. In the modern day, the research focus is shifting more and more toward intelligent cyber-physical production systems (CPPSs), which means that different production facilities are connected to some sort of a cloud computing that is capable of data collection and learning. For that shift, the machine must be aware of its environment as well as its specified job. In Zhang et al. (2022) a technique called the

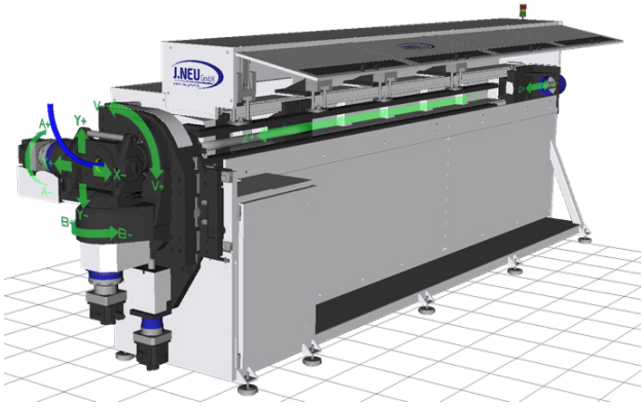

Fig. 1. 3D-Representation of the Freeform bending Machine

active deflection method (ADM) has been proposed, so that the tube being bent avoids collision with the machine construction during the bending of complex geometrical structures. For a successful implementation of a closed-loop system that also considers the geometry of the workpiece being bent, a system identification for the considered tube should take place. This was shown in previous works like Sun and Stelson (1997), where different system identification approaches based on frequency-response, the least-square method, and the singular value decomposition method were represented. Staupendahl et al. (2016) proposed a closed-loop control concept to compensate for the

⋆ This research was funded by the Deutsche Forschungsgeminschaft (DFG, German Research Foundation) - Grant number: 424334138.


10.1016/j.ifacol.2023.10.1358

Underbending2.png Underbending2.bb

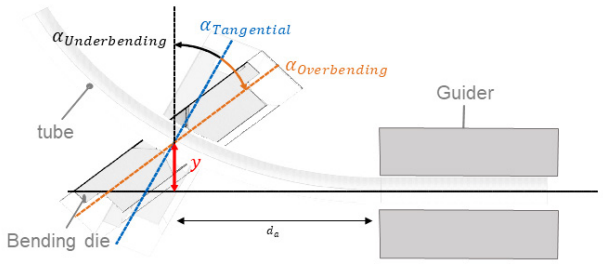


Fig. 2. Over- and Underbending

springback effect using the bending force and torque and by measuring the profile contour after bending.

These previous works, however, only considered the workpiece geometry. Ismail et al. (2021) laid the basis for a closed-loop control structure that considers the residual stresses inside the material, as well as the geometry of the workpiece. In this case, the workpiece, which is a tube with a circular cross-section, was modeled based on the kinematics of the machine and a rheological model based on a Saint-Venant element (St. Vt. element) to represent the elastic-plastic behavior of the bending process (the springback effect). Since rheological models and St. Vt. elements are not the focus of this work, they will not be explained here. However, Maier et al. (2021) showed experimentally that the same bending geometry based on the kinematics of the machine (*tangential bending*) can be also achieved by using different combinations of the translational and rotational movements of the bending die (*over- and underbending*), see Fig. 1.1. There, it was also shown that the over- and underbending has a significant effect on the residual stresses inside the tube. A mathematical formulation that decouples the residual stresses ($\sigma$) from their respective geometry (i.e., bending curvature ($\kappa$)) considering the over- and underbending phenomena was thoroughly investigated in Ismail et al. (2022). Here, the least square method was utilized for the parameter estimation of the formulation relating the translational and rotational position of the bending die together with the respective curvature ($\kappa$) and residual stresses ($\sigma$). As previously mentioned, for a successful closed-loop control structure, the machine has to be aware of its environment as well as the job being done. To that end, the basis for a soft sensor is laid in Stebner et al. (2021). This sensor estimates the value of the residual stresses without the need to destroy the workpiece itself or indent it, which enables in turn, the inline measurement of the residual stresses during the runtime of the bending process. In Stebner et al. (2022), this soft sensor is extended to include the weld seam along the longitudinally welded tube.

### *1.2 Goals of the Paper*

One of the challenges that face the bending process, from the point of view of Automatic Control Engineering, is deviation correction. In systems that are normally discussed and taught in the literature, the system states are (most of the time) continuously observed and can be immediately anticipated and compensated for. In contrast, in free-form bending processes, the system state can only be measured after the tube section has already been bent. This means that whenever a deviation occurs, it cannot be corrected anymore. In this work, an idea to overcome this problem is to be investigated. This idea is based on the previously mentioned fact that deviations that has already happened cannot be repaired anymore. However, the course path of the rest of the unbent tube can be recalculated so that the deviation propagation along the rest of the tube is reduced. This way, the desired shape can at least be preserved with minimum sacrifices. In turn, this will reduce the amount of disposed of materials due to failures during the bending process, and hence production costs as well. Another advantage for this approach, in comparison to the classic P-Controllers, is that the performance index optimization function can be so customized that reactions against large deviations are smooth, reducing material failure.

## 2. METHODOLOGY AND ASSUMPTIONS

The free-form bending machine under consideration has six degrees of freedom (DOF), namely five DOF for the bending head (two translatory in $x$ and $y$ directions, and three rotational about $x, y$, and $z$ axes) plus one DOF along the $z$ axis for the tube feeder. In previous works Ismail et al. (2021, 2022), these six DOF have been reduced to just three, namely one DOF for the tube feeder in the $z$ direction and two DOF for the bending die (one translatory along the $y$ axis and one rotary about the $x$ axis). The same assumption has been further assumed in this work. Moreover, the results of this work are based on the mathematical models and formulations depicted in Ismail et al. (2022). It is also to be noted, that the validation of the optimization algorithm is done based on MATLAB simulation software packages.

### *2.1 Introduction to the Residual Strategy Algorithm*

The main goal of the *Residual Strategy Algorithm*, is to recalculate the path of the remaining part of the unbent tube, so that the final shape and curvature $\kappa$ should - to some extent - remain preserved, even after a segment has been bent incorrectly. The definition of the curvature $\kappa$ is the rate of angular change $\partial\alpha$ along the tube $\partial l$,

$$\begin{aligned} \kappa &= \frac{\partial \alpha}{\partial l}, \\ \partial \alpha &= \kappa \, \partial l, \\ \int_0^{\alpha} \partial \alpha &= \int_0^{l} \kappa(l) \, \partial l, \\ \alpha &= \int_0^{l} \kappa(l) \, \partial l, \end{aligned} \tag{1}$$

where $l$ is the tube length considered and $\alpha$ is the bending angle of this length. The continuous tube is now to be discretized into parts of equidistant length $\Delta l$. The number of segments is determined taking into consideration the bent length $l$, as well as the minimum distance that the bending die can bend, which depends on the resolution of the machine. The number of discrete segments will be denoted by $n$, so

$$\alpha = \sum_{i=1}^{n} \kappa_i \Delta l. \tag{2}$$

Fig. 3 shows a depiction of a tube discretized into $n$ segments. Each segment has a curvature $\kappa_i$, where the index $i$ denotes the number of the discretized segment.

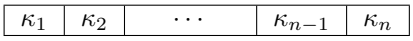


Fig. 3. The tube to be bent discretized into $n$ segments

The state of the tube can therefore be expressed in a good approximation using the $n$ curvatures $\kappa_1$, $\cdots$, $\kappa_n$ of the segments, combined into the state vector $\boldsymbol{\kappa} = [\kappa_1 \ ... \ \kappa_n]^T$.

At the beginning of the bending process, the tube is not curved, $\boldsymbol{\kappa[0]} = \mathbf{0}$, and after the entire bending process, a specified desired geometry $\boldsymbol{\kappa_{des}}$ should be implemented as accurately as possible. For the bending process, the control signals to the actuators must be set properly. As explained in Ismail et al. (2022), the bending result is related to the technical control signals in a non-linear way, and the required curvature $\boldsymbol{\kappa_{des}}$ can be specified then by applying a non-linear inverse characteristic curve (the mapping block in Fig. 4).

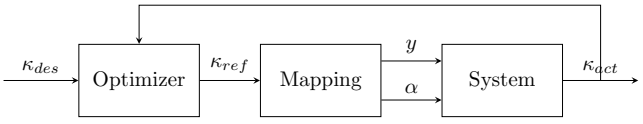


Fig. 4. Block diagram of the optimization algorithm

The bending now can be sequentially carried out from segments 1 to $n$ (these sequential steps will be denoted with the discrete-time variable $[k]$, where $k = 1 \cdots n$). When bending the first segment ($k = 1$), $\kappa_{ref}[1] = \kappa_{des,1}$ is to be chosen. Following this, the actually achieved curvature $\kappa_{act,1}$ is measured and compared to its respective desired curvature $\kappa_{des,1}$. If there is no deviation, then the second segment ($k = 2$) proceeds in the same manner. If, however, a deviation is sensed, then the planned upcoming curvatures $\kappa_{ref}[2]$ to $\kappa_{ref}[n]$ are recalculated, so that the final result will be close to the desired final shape $\boldsymbol{\kappa_{des}}$. This can be achieved by minimizing a cost or performance index function $J$. After bending the second segment, a new measurement is carried out, and the upcoming curvatures $\kappa_{ref}[3]$ to $\kappa_{ref}[n]$ must be recalculated. In other words, after each segment $k$, a new optimal residual strategy for the segments $k + 1$ to $k = n$ is calculated. From this residual strategy only the first element is introduced to the reference signal $\kappa_{ref}$, then measured and again optimized. This procedure is similar to the *Model Predictive Optimal Control* of processes Grüne (2017), but with a *shrinking horizon* for each step (*shrinking horizon model-predictive control strategy*) Skaf et al. (2010).

### *2.2 Formalization of the Optimization Problem*

The dynamical system with state vector $\boldsymbol{\kappa}$ follows the linear time-variant state difference equation:

$$\boldsymbol{\kappa[k]} = \boldsymbol{\kappa[k-1]} + \boldsymbol{e_k}\kappa_{ref}[k], \forall\, k = 1, \cdots, n. \tag{3}$$

Here $\boldsymbol{e_k}$ represents the unity vector with 1 at the $k^{th}$ position so that in the $k^{th}$ step, only the $k^{th}$ segment is acted upon (which makes the model time-variant).

For the bending of the first segment, $\kappa_{ref}[1] = \kappa_{des,1}$ is introduced to the system. After bending the $i^{th}$ segment ($i = 1, ..., n-1$), the actually achieved curvature $\kappa_{act,1}$ is measured, and the *residual strategy* $\kappa_{ref}[i+1], ..., \kappa_{ref}[n]$ is chosen so that the following performance index function is minimized:

$$J = J(\boldsymbol{\kappa_{act,1:i}}, \boldsymbol{\kappa_{ref}}[i+1:n], \boldsymbol{\kappa}_{des}). \tag{4}$$

Only $\kappa_{ref}[i+1]$ is introduced to the system for carrying out the bending of segment $i+1$. This control strategy can be denoted *model-predictive-control* on a shrinking horizon. Fig. 5 shows a pseudo-code for the previously described procedure.

Residual-Strategy Algorithm:

- `Read` $\boldsymbol{\kappa_{des}}, \boldsymbol{\kappa_{act}}$.
- `Bend the first segment.`

`for i=1:n-1`

$$\min_{\boldsymbol{\kappa_{ref}}} \quad J(\boldsymbol{\kappa_{act,1:i}}, \boldsymbol{\kappa_{ref}}[i+1:n], \boldsymbol{\kappa}_{des}) \tag{5}$$

$Apply \kappa_{ref,i+1}$
$Bend the following segment$ `i+1`.
$Measure and update \kappa_{act,i+1}$
`end`

Fig. 5. Pseudo-Code for the Residual Strategy Algorithm

### *2.3 Choice of the Performance Index Function*

The choice of the performance index function is, to a great extent, left to the user, taking into account the respective technical requirements. For example, the absolute value of the total curvature error can be approached so that the sum of actually reached angles of all segments complies with that of the desired geometry,

$$J_1 = |\sum_{j=1}^{n}(\kappa_j - \kappa_{des,j})|, \tag{6}$$

where $\kappa_j$ denotes $\kappa_{act,j}$ for the already bent segments, and denotes $\kappa_{ref}[j]$ for those still to be bent.

In order to give a particular attention to the upcoming curvatures, the squared deviation from the desired curvature is considered. This is multiplicated then with the term $i^3$ which corresponds to the index value of the current segment. The goal behind this, is to increase the weighting as the bending process gets closer to the end.

$$J_2 = (\sum_{i}^{n}(\kappa_{ref,i} - \kappa_{des,i})^2) * i^3. \tag{7}$$

In order to guarantee a smooth transition between previous and current segments, the difference between the curvature of the previous and current segments is deduced from that of the desired curvature.

$$J_3 = ((\kappa_{act,i-1} - \kappa_{ref,i}) - (\kappa_{des,i-1} - \kappa_{des,i}))^2. \tag{8}$$

In practice, it is advisable to strive for a compromise between these requirements in the form:

$$J = w_1 J_1 + w_2 J_2 + w_3 J_3, \tag{9}$$

where $w_1$, $w_2$, and $w_3$ are the elements of the weighting vector $\boldsymbol{w}$.

## 3. SIMULATION RESULTS

The previous residual strategy optimization algorithm was implemented and tested using the `fmincon()` library package provided by MATLAB. For the simulation, various bending scenarios were considered with different weighting factors. In the first scenario, Fig. 6, a total bending angle $\alpha = 90° \approx 1.57rad$ was desired. The total length of the tube to be bent was $l = 1000mm$, while the number $n$ of discretized segments was 20. The upper part of Fig. 6 shows the desired curvature course (in red). After a length of $\approx 150mm$, a continuous offset perturbation was added in order to test the optimization algorithm. This kind of perturbation can be similar to some extent to false machine settings in practice. In yellow, the curvature path of the tube without recalculating the optimal course can be seen. The blue curve shows the curvature path followed upon applying the optimization algorithm. The bottom part of Fig. 7 shows the depicted 2D shape of the paths of different bending scenarios compared to the desired path. It can be easily inferred that the optimized residual strategy path has, in this case, to a significant extent, preserved the final desired bent shape of the tube. In this case, the weighting vector $\boldsymbol{w}$ of the performance index function $J$ depicted in (9) is $[w_1, w_2, w_3] = [10.0, 25.0, 0.1]$.

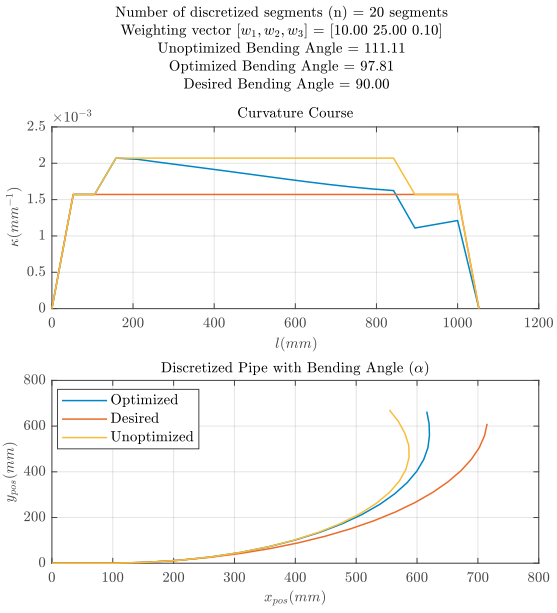


Fig. 6. Course of desired, optimized, and unoptimized curvatures with $w_1 = 10$, and bending angle $(\alpha) = 90°$

As previously mentioned in equations (6), (7), and (8), $w_1$ refers to the weighting of the total bending angle in compliance with previous bent and upcoming unbent segments, whereas $w_2$ implies the weighting for the upcoming unbent segments, which increases as the bending process gets closer to the last segment. $w_3$ however, is the weighting for the smoothness of the transition between current segment to be bent and the previous segment that had already been bent. Hence, avoiding sudden abrupt changes in curvature, which otherwise would cause failure in the workpiece. In Fig. 6, $w_1$ has a value of 10, the total bending angle of

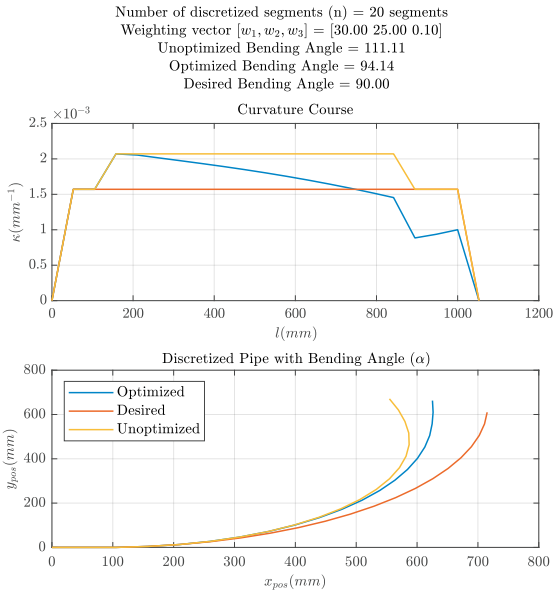


Fig. 7. Course of desired, optimized, and unoptimized curvatures with $w_1 = 30$, and bending angle $(\alpha) = 90°$

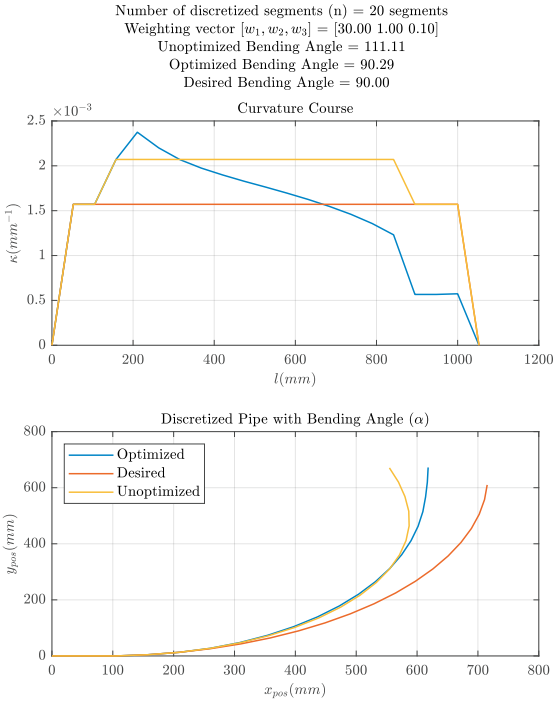


Fig. 8. Course of the desired, optimized, and unoptimized Curvature with $w_2 = 1$ and bending angle $(\alpha) = 90°$

the optimized trajectory hereby was 97.81°, whereas that of the unoptimized one was 111.11°. Upon increasing the value of $w_1$ to a value of 30, the total bending angle of the optimized trajecotry was reduced to 94.14° and got closer to the desired bending angle as in Fig. 7.

In Fig. 8 the value of $w_2$ was reduced to 1. Here it can be seen that the total bending angle of the optimized trajectory tends to be more closer to its desired respective.

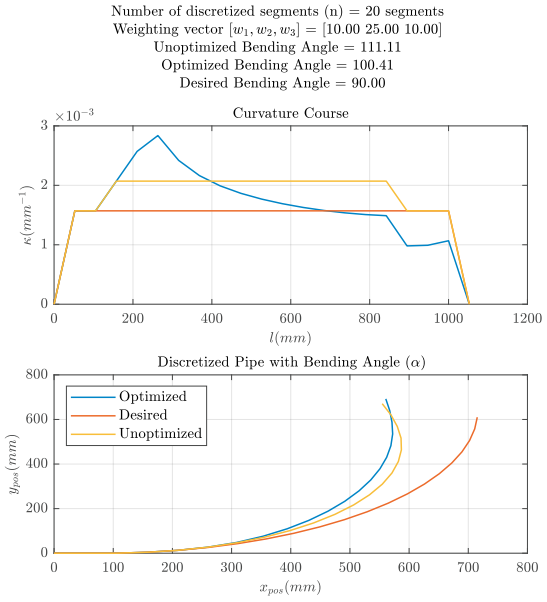


Fig. 9. Course of the desired, optimized, and unoptimized Curvature with $w_3 = 10$ and bending angle $(\alpha) = 90°$

However, the optimizer is not trying anymore to stick to the desired curvature. This can be seen at the position, where the offset was introduced, as the optimizer did not try to get closer to the desired curvature as in the previous cases. The optimizer hereby was rather concerned with keeping the total area under the curve (the total bending angle) sustained with that of the desired course.

In Fig. 9 the value of $w_3$ was increased to a value of 10. Thus increasing the smoothness with which the curvature changes. However, at the cost of the total bent angle and the coincidence with the course of the desired curvature. i.e. the optimizer is giving less effort towards compensating the deviation, rather than making sure that the change in curvature stays as smooth as possible. That can be seen if the course of the curvature at $l = 200mm$ in Fig. 9 is compared with that of Fig. 6. Here, the curvature did not change its course immediately as in Fig. 6, it kept, however, its direction temporarily until the index in 7 had increased and amplified in turn the effect of the weighting factor $w_2$. This is when the optimizer decided finally to change the course being followed and strived towards the desired curvature course.

In Fig. 10 a noisy perturbation was introduced at the end of the bending process in order to test the robustness of the algorithm against. The noisy perturbation can arise due to inconsistency in material properties along the tube, or due to the method with which the tube was manufactured; i.e. tubes could have been flat sheets before being rolled and welded. Here, it could be inferred that the optimizer could to some extent improve the total bending angle of the tube. The compliance of the total bent with its desired could be significantly improved by increasing the value of weighting factor $w_1$ as shown in Fig. 11. Here, the curvature of the last segment reached a value of $\approx 2.55 * 10^{-3} mm^{-1}$, whereas that of the last segment in Fig. 10 had a curvature of almost $2 * 10^{-3} mm^{-1}$.

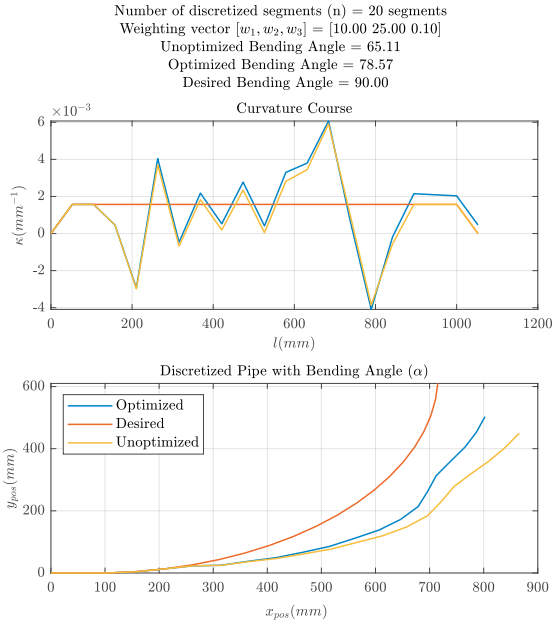


Fig. 10. Course of the desired, optimized, and unoptimized Curvatures and bending angle $(\alpha) = 90°$ upon subjection to noisy perturbations

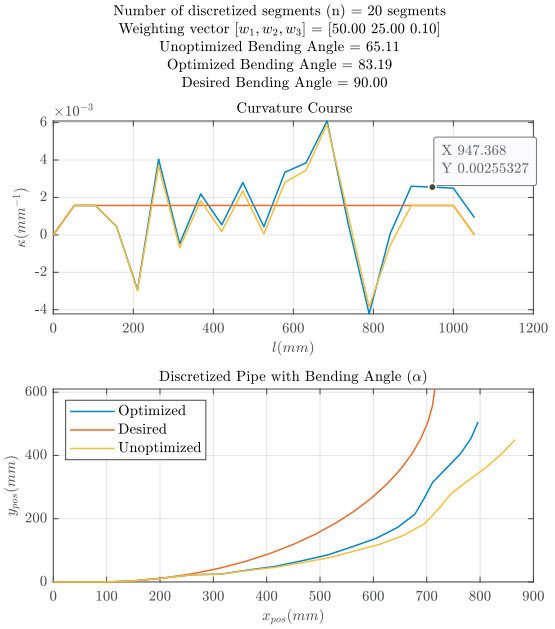


Fig. 11. Course of the desired, optimized, and unoptimized Curvatures after increasing $w_1$

## 4. CONCLUSION

This work sets the basis for an algorithm that, based on mathematical models depicted in Ismail et al. (2022), predicts the upcoming progress of the curvature of a tube being subjected to perturbations during the bending process. The results have been verified using MATLAB simulation software. It could be shown that the optimization algorithm can, based on the weight vector, significantly affect the final shape of the considered tube. The choice of the performance index function together with the weighting vector can be modified in order to accommodate

the varying technical needs and challenges of different situations. One advantage to this approach is that the predicted course can be seen and tested against different disturbances and perturbations before applying it to the real machine, and accordingly adjust the weighting vector or even the performance function until a suitable course is reached.

The simulation results could show that the optimizer can be used in noisy situations and still to some extent improve the end result. This can be further improved in upcoming works, by means of measuring the mechanical properties of the tube as in Stebner et al. (2021) before starting the bending process, and then feeding these information to the optimizer to be taken into consideration during calculating the next steps.

In the upcoming works, this residual strategy optimization algorithm should be tested experimentally under other different conditions (e.g., various materials). Moreover, more optimization goals can be added other than the geometry. I.e., the mechanical properties of the tubes (e.g., residual stresses) can also be taken into consideration after equipping the mathematical model in Ismail et al. (2022) with the soft sensor for residual stresses depicted in Stebner et al. (2021, 2022).

## REFERENCES


Ahn, K., Lee, K.H., Lee, J.S., Won, C., and Yoon, J. (2020). Analytic springback prediction in cylindrical tube bending for helical tube steam generator. *Nuclear Engineering and Technology*, 52(9), 2100–2106. doi: 10.1016/j.net.2020.02.004.

Grüne, L. (2017). *Nonlinear Model Predictive Control: Theory and Algorithms*. Communications and Control Engineering. Springer International Publishing, Cham, 2nd ed. 2017 edition. doi:10.1007/978-3-319-46024-6.

Huang, T., Wang, K., Zhan, M., Guo, J., Chen, X., Chen, F., and Song, K. (2019). Wall thinning characteristics of ti-3al-2.5v tube in numerical control bending process. *Journal of Shanghai Jiaotong University (Science)*, 24(5), 647–653. doi:10.1007/s12204-019-2079-1.

Ismail, A., Maier, D., Stebner, S., Volk, W., Münstermann, S., and Lohmann, B. (2021). A structure for the control of geometry and properties of a freeform bending process. *IFAC-PapersOnLine*, 54(11), 115–120. doi: 10.1016/j.ifacol.2021.10.060.

Ismail, A., Maier, D., Stebner, S., Volk, W., Münstermann, S., and Lohmann, B. (2022). Control system design for a semi-finished product considering over- and underbending. In *The 28th Saxon Conference on Forming Technology SFU and the 7th International Conference on Accuracy in Forming Technology ICAFT*, 16. MDPI, Basel Switzerland. doi:10.3390/engproc2022026016.

Maier, D., Stebner, S., Ismail, A., Dölz, M., Lohmann, B., Münstermann, S., and Volk, W. (2021). The influence of freeform bending process parameters on residual stresses for steel tubes. *Advances in Industrial and Manufacturing Engineering*, 2, 100047. doi: 10.1016/j.aime.2021.100047.

Skaf, J., Boyd, S., and Zeevi, A. (2010). Shrinking-horizon dynamic programming. *International Journal of Robust and Nonlinear Control*, 20(17), 1993–2002. doi: 10.1002/rnc.1566.

Staupendahl, D., Chatti, S., and Tekkaya, A.E. (2016). Closed-loop control concept for kinematic 3d-profile bending. AIP Conference Proceedings, 150002. Author(s). doi:10.1063/1.4963542.

Stebner, S.C., Maier, D., Ismail, A., Balyan, S., Dölz, M., Lohmann, B., Volk, W., and Münstermann, S. (2021). A system identification and implementation of a soft sensor for freeform bending. *Materials*, 14(16), 4549. doi:10.3390/ma14164549. URL `https://www.mdpi.com/1996-1944/14/16/4549`.

Stebner, S.C., Maier, D., Ismail, A., Dölz, M., Lohman, B., Volk, W., and Münstermann, S. (2022). Extension of a simulation model of the freeform bending process as part of a soft sensor for a property control. *Key Engineering Materials*, 926, 2137–2145. doi:10.4028/p-d17700.

Sun, W.C. and Stelson, K.A. (1997). System identification and adaptive control of the multi-axis bending and twisting process. *Journal of Dynamic Systems, Measurement, and Control*, 119(4), 782–790. doi: 10.1115/1.2802391.

Zhang, H., El-Aty, A.A., Tao, J., Guo, X., Zheng, S., and Cheng, C. (2022). Effect of active deflection on the forming of tubes manufactured by 3d free bending technology. *Metals*, 12(10), 1621. doi:10.3390/met12101621.